ORIGINAL RESEARCH

Endogenous and Therapeutic 25-Hydroxycholesterols May Worsen Early SARS-CoV-2 Pathogenesis in Mice

Michael B. Fessler[1]*, Jennifer H. Madenspacher[1], Paul J. Baker[5], Kerry L. Hilligan[6‡], Andrea C. Bohrer[5], Ehydel Castro[5], Julie Meacham[1], Shih-Heng Chen[2], Reed F. Johnson[7], Jeffrey G. McDonald[8,9], Negin P. Martin[2], Charles J. Tucker[3], Debabrata Mahapatra[10], Mark Cesta[4], and Katrin D. Mayer-Barber[5]*

[1]Immunity, Inflammation and Disease Laboratory, [2]Viral Vector Core Facility, Neurobiology Laboratory, [3]Fluorescence Microscopy and Imaging Center, Signal Transduction Laboratory, and [4]Division of the National Toxicology Program, National Institute of Environmental Health Sciences, National Institutes of Health, Research Triangle Park, North Carolina; [5]Inflammation and Innate Immunity Unit, [6]Immunobiology Section, and [7]SARS-CoV-2 Virology Core, Laboratory of Viral Diseases, National Institute of Allergy and Infectious Diseases, National Institutes of Health, Bethesda, Maryland; [8]Department of Molecular Genetics and [9]Center for Human Nutrition, University of Texas Southwestern Medical Center, Dallas, Texas; and [10]Integrated Laboratory Systems, LLC, Research Triangle Park, North Carolina

Abstract

Oxysterols (i.e., oxidized cholesterol species) have complex roles in biology. 25-Hydroxycholesterol (25HC), a product of the activity of cholesterol-25-hydroxylase (CH25H) on cholesterol, has recently been shown to be broadly antiviral, suggesting therapeutic potential against severe acute respiratory syndrome coronavirus 2 (SARS-CoV-2). However, 25HC can also amplify inflammation and be converted by CYP7B1 (cytochrome P450 family 7 subfamily B member 1) to 7α,25-dihydroxycholesterol, a lipid with chemoattractant activity, via the G protein–coupled receptor EBI2 (Epstein-Barr virus–induced gene 2)/GPR183 (G protein–coupled receptor 183). Here, using *in vitro* studies and two different murine models of SARS-CoV-2 infection, we investigate the effects of these two oxysterols on SARS-CoV-2 pneumonia. We show that although 25HC and enantiomeric-25HC are antiviral *in vitro* against human endemic coronavirus-229E, they did not inhibit SARS-CoV-2; nor did supplemental 25HC reduce pulmonary SARS-CoV-2 titers in the K18-human ACE2 (angiotensin-converting enzyme 2) mouse model *in vivo*. Treatment with 25HC also did not alter immune cell influx into the airway, airspace cytokines, lung pathology, weight loss, symptoms, or survival but was associated with increased airspace albumin, an indicator of microvascular injury, and increased plasma proinflammatory cytokines. Conversely, mice treated with the EBI2/GPR183 inhibitor NIBR189 displayed a modest increase in lung viral load only at late time points but no change in weight loss. Consistent with these findings, although *Ch25h* and 25HC were upregulated in the lungs of SARS-CoV-2–infected wild-type mice, lung viral titers and weight loss in *Ch25h*$^{-/-}$ and *Gpr183*$^{-/-}$ mice infected with the β variant were similar to those in control animals. Taken together, endogenous 25HCs do not significantly regulate early SARS-CoV-2 replication or pathogenesis, and supplemental 25HC may have proinjury rather than therapeutic effects in SARS-CoV-2 pneumonia.

Keywords: 25-hydroxycholesterol; cholesterol-25-hydroxylase; pneumonia; EBI2; SARS-CoV-2

(Received in original form January 5, 2023; accepted in final form August 14, 2023)

*These authors contributed equally to this work.

‡Present address: Malaghan Institute of Medical Research, Wellington, New Zealand.

Supported by Division of Intramural Research, National Institute of Allergy and Infectious Diseases grant Z01 AI00129303, National Institute of Environmental Health Sciences Intramural Research Program grants Z01 ES102005 and ES103316, CTSA UL1TR003163, National Institute of Diabetes and Digestive and Kidney Diseases grant 5P01HL160487, and National Heart, Lung, and Blood Institute grant 1P30DK127984.

Author Contributions: Study design, data analysis, and writing: M.B.F. and K.D.M.-B. Study design, data collection and analysis, and manuscript revision: J.H.M., P.J.B., K.L.H., A.C.B., E.C., J.M., S.-H.C., R.F.J., J.G.M., N.P.M., C.J.T., D.M., and M.C.

Correspondence and requests for reprints should be addressed to Katrin D. Mayer-Barber, Ph.D., National Institute of Allergy and Infectious Diseases, Building 33, Room 2W10.A3, 33 North Drive, MSC 3206, Bethesda, MD 20892. E-mail: mayerk@niaid.nih.gov.

This article has a related editorial.

This article has a data supplement, which is accessible from this issue's table of contents at www.atsjournals.org.

Am J Respir Cell Mol Biol Vol 69, Iss 6, pp 638–648, December 2023

Originally Published in Press as DOI: 10.1165/rcmb.2023-0007OC on August 14, 2023
Internet address: www.atsjournals.org

Clinical Relevance

Oxysterols have recently been identified as antiviral, raising interest in them as potential therapeutics against coronavirus disease (COVID-19). Here, we provide evidence that 25-hydroxycholesterol is antiviral against human endemic coronavirus-229E but does not exhibit appreciable activity against severe acute respiratory syndrome coronavirus 2 (SARS-CoV-2) either *in vitro* or *in vivo*. Instead, animals treated with 25-hydroxycholesterol in the context of SARS-CoV-2 pneumonia display evidence of exacerbated pulmonary vascular injury.

In 2013, two groups identified 25-hydroxycholesterol (25HC), an oxysterol product of the enzyme cholesterol-25-hydroxylase (CH25H), as broadly antiviral (1, 2). All enveloped viruses tested to date, among them influenza A, herpes simplex virus 1, varicella zoster virus, murine γ herpes virus, human immunodeficiency virus (HIV), vesicular stomatitis virus, hepatitis viruses B and C, and Ebola virus, are inhibited by 25HC, with half maximal inhibitory concentrations in the nanomolar to low micromolar range (3). 25HC blocks viral fusion by modifying host cell membranes and potentially by inhibiting the lipogenic transcription factor SREBP-2 (sterol regulatory element–binding protein 2) (3). Additional posited mechanisms include effects on virus capsid disassembly, genome replication, protein expression, and cellular egress (2).

CH25H is expressed by airway epithelium (4) and alveolar macrophages (5, 6) in mice and humans and induces robust extracellular release of 25HC after upregulation by virus and IFNs (1). Systemic treatment with exogenous 25HC to augment this native response effectively treats viral infections, including pneumonia, in mice, pigs, and nonhuman primates (2, 7, 8). Moreover, exogenous 25HC is antiinflammatory through inhibition of inflammasomes (9) and accelerates the resolution of lung inflammation in mice through activation of LXR (liver X receptor) (5). Reports such as these have collectively suggested potential for 25HC as a therapeutic for viral pneumonia. However, other reports that 25HC amplifies proinflammatory signaling and that *Ch25h*$^{-/-}$ mice have attenuated lung pathology during influenza A pneumonia (10) have suggested possible untoward effects of 25HC *in vivo*. Further complicating questions of mechanism, 25HC is converted by the enzyme CYP7B1 (cytochrome P450 family 7 subfamily B member 1) into 7α,25-dihydroxycholesterol (7α,25HC), a ligand for EBI2 (Epstein Barr virus–induced gene 2; encoded by *Gpr183*), a G protein–coupled receptor that can promote migration of several immune cell types to the lung (4, 6, 11, 12).

Of interest, it was recently reported that 25HC inhibits severe acute respiratory syndrome coronavirus 2 (SARS-CoV-2) infection in cell lines (13–17). One group also reported that treatment of mice with 25HC reduced lung viral load 3 days postinfection (p.i.) with mouse-adapted SARS-CoV-2, but no further outcomes were presented (16), leaving many questions unaddressed. Here, we show that although both 25HC and enantiomeric-25HC (ent-25HC) inhibit cellular infection by endemic human coronavirus (hCoV)–229E, they failed to limit SARS-CoV-2 infection. Moreover, during *in vivo* SARS-CoV-2 infections, *Ch25h*-deficient mice were able to control viral replication, and transgenic mice expressing hACE2 (human angiotensin-converting enzyme 2) under the epithelial K18 promotor (K18-ACE2 mice) treated with supplemental 25HC did not exhibit changes in viral titers. Treatment with 25HC had no effect on airway immune response, lung histopathology, morbidity, or mortality but did increase plasma chemokines as well as BAL fluid (BALF) albumin, a metric of microvascular injury (18). *Gpr183*-deficient mice displayed no significant changes in lung viral loads or weight loss, thus arguing against a role for the downstream lipid 7α,25HC. Taken together, our findings suggest that 25HC is not therapeutic during SARS-CoV-2 pneumonia and that GPR183 and CH25H are dispensable for early viral control *in vivo*. Some of the results of these studies have been previously reported in preprint form (https://www.biorxiv.org/content/10.1101/2022.09.12.507671v1.full).

Methods

Reagents

25HC was acquired from Sigma-Aldrich, and ent-25HC was custom synthesized by Avanti Polar Lipids. The GPR183-specific antagonist NIBR189 was acquired from Tocris (Bio-Techne).

Mice

Male and female B6.Cg-Tg(K18-ACE2)2Prlmn/J (#034860; The Jackson Laboratory), C57BL/6 (B6; The Jackson Laboratory), *Ch25h*$^{-/-}$ (#016263; the Jackson Laboratory) (5), and *Gpr183*$^{-/-}$ (19) (kindly provided by Vanja Lazarevic) mice, ∼22–26 g in weight, were used. The light/dark cycle was set at 12/12 hours, and mice were fed Purina Lab Diet #5002 and provided water *ad libitum*. Animal care and housing met Association for Assessment and Accreditation of Laboratory Animal Care International guidelines, the Guide for Care and Use of Laboratory Animals (National Research Council), and requirements as stated by the U.S. Department of Agriculture through the Animal Welfare Act. All experiments were performed in compliance with an animal study proposal approved by the National Institute of Allergy and Infectious Diseases (NIAID) Animal Care and Use Committee or the National Institute of Environmental Health Sciences Animal Care and Use Committee.

In Vivo Murine SARS-COV2 Viral Infections and Treatments

In some studies, K18-hACE2 mice were treated intraperitoneally with 50 mg/kg 25HC or vehicle (hydroxypropyl-beta-cyclodextrin; Cyclo Therapeutics, Inc.) at −4 hours in relation to viral infection, and every 24 hours thereafter until sacrifice. In other studies, K18-hACE2 mice were intraperitoneally injected with 0.1 or 0.5 mg/kg NIBR189 on days −1, +1, and +3 p.i. K18-hACE2 mice were infected intranasally with 35 μl neat USA-WA1/2020 SARS-CoV-2 (BEI Resources), with a target dose of 1+E03 median tissue culture infectious dose ($TCID_{50}$) per mouse. SARS-CoV-2 USA-WA-1 (WA1/2020), GenBank MN985325.1, was propagated on Vero E6 TMPRSS2 (serine protease 2) cells (20). The virus sequence was confirmed using Illumina sequencing and did not differ from the parental virus, except for S6L in E, T7I in M, and S194T in N (virus used in 25HC treatment experiments) and for the following SNPs compared with reference sequence: C23525T, C26261T, C26542T, and T28853A (virus used in NIBR189 experiments). All experiments with SARS-CoV-2 were

performed at Biosafety Level 3. B6, *Ch25h*$^{-/-}$, and *Gpr183*$^{-/-}$ mice were infected intranasally with 3.5×10^4 $TCID_{50}$ SARS-CoV-2 hCoV-19/South Africa/KRISP-K005325/2020 β variant of concern (Pango lineage B.1.351, Global Initiative on Sharing All Influenza Data reference EPI_ISL_860618, BEI Resources) in 35 μl. Exposure doses were confirmed by $TCID_{50}$ assay of remaining stock in Vero E6 cells (CRL-1586; American Type Culture Collection). Before inoculation, mice were anesthetized with ketamine (80–100 mg/kg) and xylazine (5–10 mg/kg) or isoflurane.

Mass Spectrometric Quantitation of Oxysterols

25HC was quantified as previously described (21). Briefly, 25HC was extracted from lung with organic solvents and quantified using a 4000 QTRAP liquid chromatography mass spectrometer (Applied Biosystems) (22).

Statistical Analysis

Analysis was performed using GraphPad Prism software. Data are represented as mean ± SEM. Two-tailed Student's *t* tests were applied for comparisons of two groups and ANOVA for comparisons of more than two groups. Survival was evaluated using the log-rank test. For all tests, *P* values <0.05 were considered to indicate statistical significance.

Additional methods can be found in the data supplement.

Results

25HC Inhibits Human Endemic Coronavirus Infection but Not SARS-CoV-2 *In Vitro*

25HC is broadly antiviral against enveloped viruses, reportedly inhibiting virus fusion by altering the cholesterol content of the host cell membrane (3). 25HC may sterically redistribute free cholesterol by incorporation into host membranes, although it has also been posited to reduce membrane free cholesterol through activation of the enzyme acyl-coenzyme A:cholesterol acyltransferase (17). Specific protein-binding interactions are typically not preserved in enantiomeric versions of lipids (1). We started with testing 25HC for efficacy against a common-cold coronavirus. To distinguish the mode of mechanism, we pretreated MRC-5 cells with 25HC, ent-25HC, or vehicle and then infected them with the endemic hCoV-229E. As shown in Figure 1A, 25HC and ent-25HC both significantly reduced viral plaque number, with 25HC exhibiting a much more robust effect. 25HC and ent-25HC also reduced plaque size, suggestive of postentry effects on replication (1), with 25HC again displaying a more marked effect (Figure 1B). Taken together, these findings suggest that 25HC antagonizes hCoV-229E through both protein binding–dependent and protein binding–independent mechanisms.

We next tested 25HC and ent-25HC for antagonism against SARS-CoV-2 USA-WA-1 in Vero E6 cells stably transfected with TMPRSS2. Contrary to the case with hCoV-229E, neither 25HC nor ent-25HC exhibited a significant effect on SARS-CoV-2 replication at concentrations up to 10 μM, as indicated by both plaque reduction assay and yield reduction assay (Figures 1C and E1A in the data supplement). Similarly, 25HC did not significantly reduce the plaque number of SARS-CoV-2 β variant B.1.351 (*see* Figure E1B). In contrast, remdesivir inhibited SARS-CoV-2 USA-WA-1 in a dose-dependent manner, confirming the robustness of the assay (Figure 1D). Although we also wished to test 25HC efficacy against hCoV-229E in Vero E6/TMPRSS2 cells, we were unable to do so, as we did not detect viral plaque formation out to 9 days p.i., even with a 10-fold higher viral inoculum (data not shown), consistent with prior reports of the nonpermissiveness of these cells to hCoV-229E (23).

Neither Native CH25H nor Exogenous 25HC Alters Viral Replication in Lungs of SARS-CoV-2–infected Mice

We next tested the roles of CH25H and 25HC in pulmonary host defense against SARS-CoV2 *in vivo*. *Ch25h* was robustly upregulated in the lungs of K18-hACE2 transgenic mice (24) at 48 and 72 hours p.i. (Figures 2A and 2B) with SARS-CoV-2 USA-WA1. At 120 hours p.i., 25HC was induced in the lungs of K18-hACE2 mice but not B6 mice (Figure 2C), used as a negative control for infection with SARS-CoV-2 USA-WA1. To test the impact of *Ch25h* deletion, *Ch25h*$^{-/-}$ mice and wild-type (WT) (B6) control animals were next infected with SARS-CoV-2 β variant (B.1.351) (Figure 2D). B.1.351 virus induced a robust increase in 25HC in the lungs of B6 mice (*see* Figure E2). Despite a numerical reduction in lung 25HC in infected *Ch25h*$^{-/-}$ mice compared with control animals (Figure 2E), *Ch25h*$^{-/-}$ mice had equivalent viral load in the lungs (Figure 2F) and equivalent weight loss at 72 hours p.i. (Figure 2G).

To test whether supplemental 25HC might nonetheless have antiviral effect *in vivo* during SARS-CoV-2 pneumonia, we treated K18-hACE2 transgenic mice intraperitoneally with 50 mg/kg/d 25HC (or vehicle), a 25HC dosing regimen that has been reported to be antiviral against HIV and Zika virus in mice (2, 7) and to accelerate resolution of lung inflammation in mice (5) (Figure 3A). We confirmed that this regimen significantly increased 25HC in lung homogenates of naive K18-hACE2 transgenic mice (Figure 3B). However, exogenous 25HC, compared with vehicle, did not significantly alter viral load in the lung, as assessed either using quantitative PCR or plaque assay (Figures 3C and 3D), nor did it modify clinical symptom scores or weight loss (*see* Figure E3).

25HC Does Not Modify the Pulmonary Immune Response to SARS-CoV-2

SARS-CoV-2, like other respiratory viruses, induces a time-dependent cellular immune response in the lungs (24). It is believed that acute lung injury, morbidity, and mortality during SARS-CoV-2 pneumonia stem largely from an overexuberant inflammatory response (24). Given this, we next profiled the pulmonary immune response of infected mice to investigate possible effects of 25HC. Total airway cell count in the BAL, as well as BALF concentrations of multiple proinflammatory cytokines and chemokines, were all unchanged by 25HC treatment at 48–72 hours p.i. (Figures 4A and 4B). In contrast, several chemokines were elevated in the plasma of 25HC-treated mice 120 hours p.i. (Figure 4C), a time point by which morbidity and mortality have commenced in this model (24) (Figures 5D and E3). Taken together, these findings indicate that treatment with 25HC alters neither viral clearance nor the immune/inflammatory response to SARS-CoV-2 in the mouse lung but may be associated with elevated systemic concentrations of proinflammatory chemokines at later time points.

25HC Does Not Attenuate SARS-CoV-2–induced Lung Pathology and Increases Microvascular Leak

SARS-CoV-2 induces severe acute lung injury that can lead to respiratory failure and death (24). Pulmonary vascular damage is a prominent feature of the pathogenesis and is

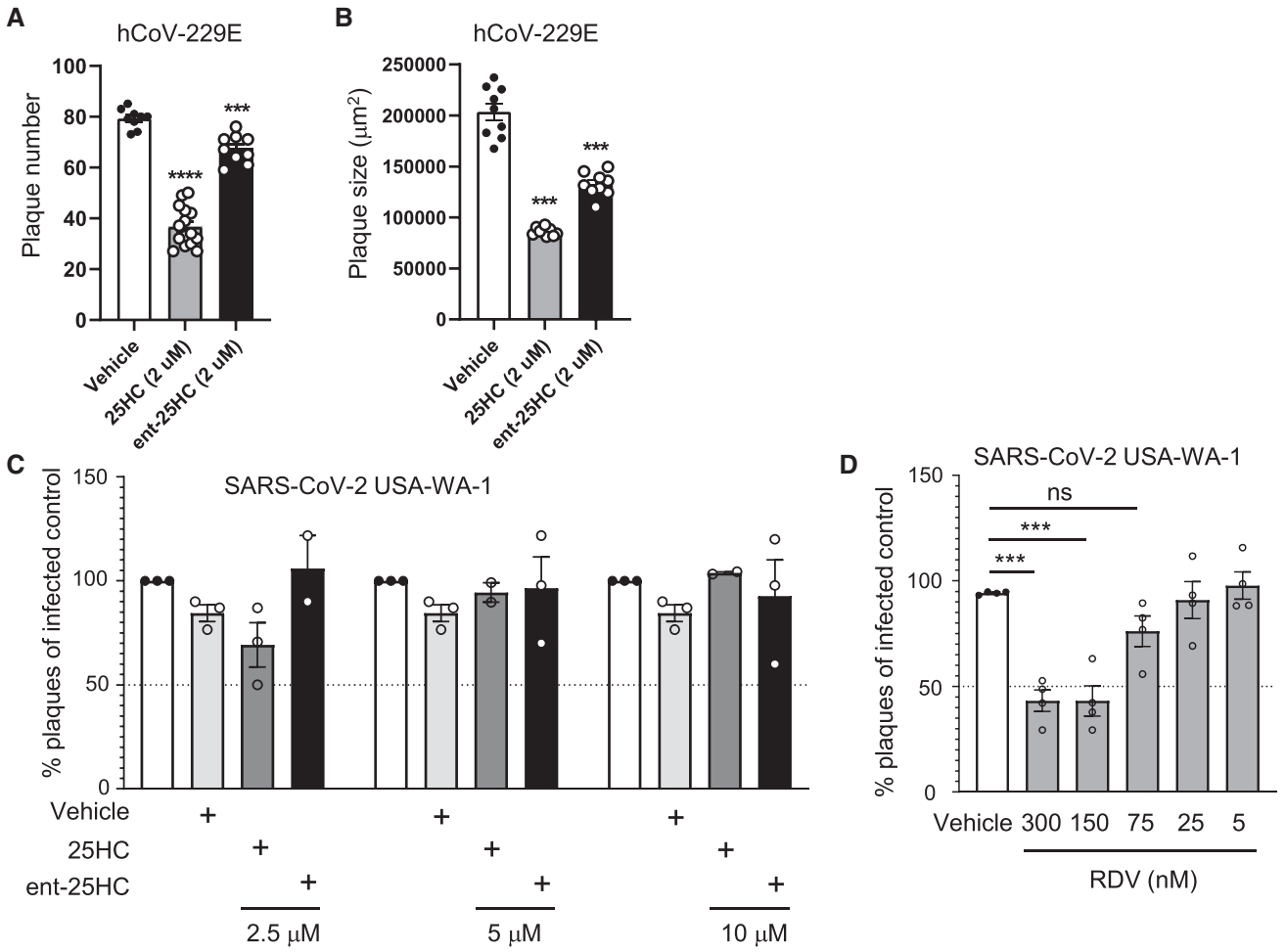

Figure 1. 25-Hydroxycholesterol (25HC) antagonizes coronavirus infection *in vitro*. (*A* and *B*) MRC-5 cells were treated with 2 μM 25HC, 2 μM ent-25HC, or vehicle overnight; infected with hCoV-229E; and then evaluated for plaque number (*A*) and plaque size (*B*). (*C*) TMPRSS2 (transmembrane serine protease 2)–expressing Vero E6 cells were treated overnight with the indicated concentrations of oxysterols or vehicle, infected with SARS-CoV-2, and then evaluated for plaque number. (*D*) As a positive control to confirm assay performance, RDV at a range of concentrations was tested for viral plaque reduction under the same conditions as in *C*. Data are mean ± SEM and are representative of two or three independent experiments. ***$P < 0.001$, and ****$P < 0.0001$. ent-25HC = enantiomeric 25-hydroxycholesterol; hCoV = human coronavirus; ns = not significant; RDV = remdesivir; SARS-CoV-2 = severe acute respiratory syndrome coronavirus 2.

believed to arise from direct viral infection or stimulation of endothelium (25). We found that by 72–120 hours p.i., the lungs of K18-hACE2 transgenic infected mice exhibited severe neutrophilic and mononuclear cell infiltration that was associated with septal thickening, type II alveolar epithelial cell hyperplasia, airway epithelial cell hyperplasia, and focal necrosis and hemorrhage (Figure 5A). Comparable lung histopathology was observed in the lungs of vehicle- and 25HC-treated mice (Figures 5A and 5B). Of interest, 25HC-treated mice had elevated BALF concentrations of albumin (Figure 5C), an established metric of pulmonary microvascular injury (18). Regardless, 25HC had no effect on mortality (Figure 5D). Collectively, these findings suggest that supplemental 25HC does not overtly modify cellular histopathology in the lungs and has no effect on survival but may aggravate damage to the alveolocapillary barrier during SARS-CoV-2 pneumonia.

Neither Deletion nor Pharmacological Inhibition of *Gpr183*/EBI2 Alters Host Defense after SARS-CoV-2 Infection

After biosynthesis by CH25H, 25HC is converted by the enzyme CYP7B1 into 7α,25HC, an oxysterol ligand for EBI2 (encoded by *Gpr183*) (26). EBI2 is expressed by multiple leukocyte types and is believed to induce the migration of Gpr183-expressing immune cells to the lung in response to 7α,25HC induced by allergens, cigarette smoke, and *Mycobacterium tuberculosis* (4, 6, 11, 12). Concentrations of 7α,25HC are deficient in *Ch25h*$^{-/-}$ mice (27). Given that *in vivo* studies of CH25H and 25HC may be confounded by downstream processing of 25HC into 7α,25HC (27, 28), we next investigated EBI2 in two models of SARS-CoV-2 pneumonia. First, *Gpr183*-null mice and WT control animals were infected with SARS-CoV-2 B.1.351 (β variant). Equivalent lung viral loads were found in both genotypes on Day 3 p.i. (Figure 6A). Second, K18-hACE2 transgenic mice were treated with the EBI2 antagonist NIBR189 or vehicle and infected with SARS-CoV-2-WA1/2020. Treatment with 0.1 mg/kg NIBR189, a dose previously reported to be well tolerated for repeated treatments and pulmonary mode of

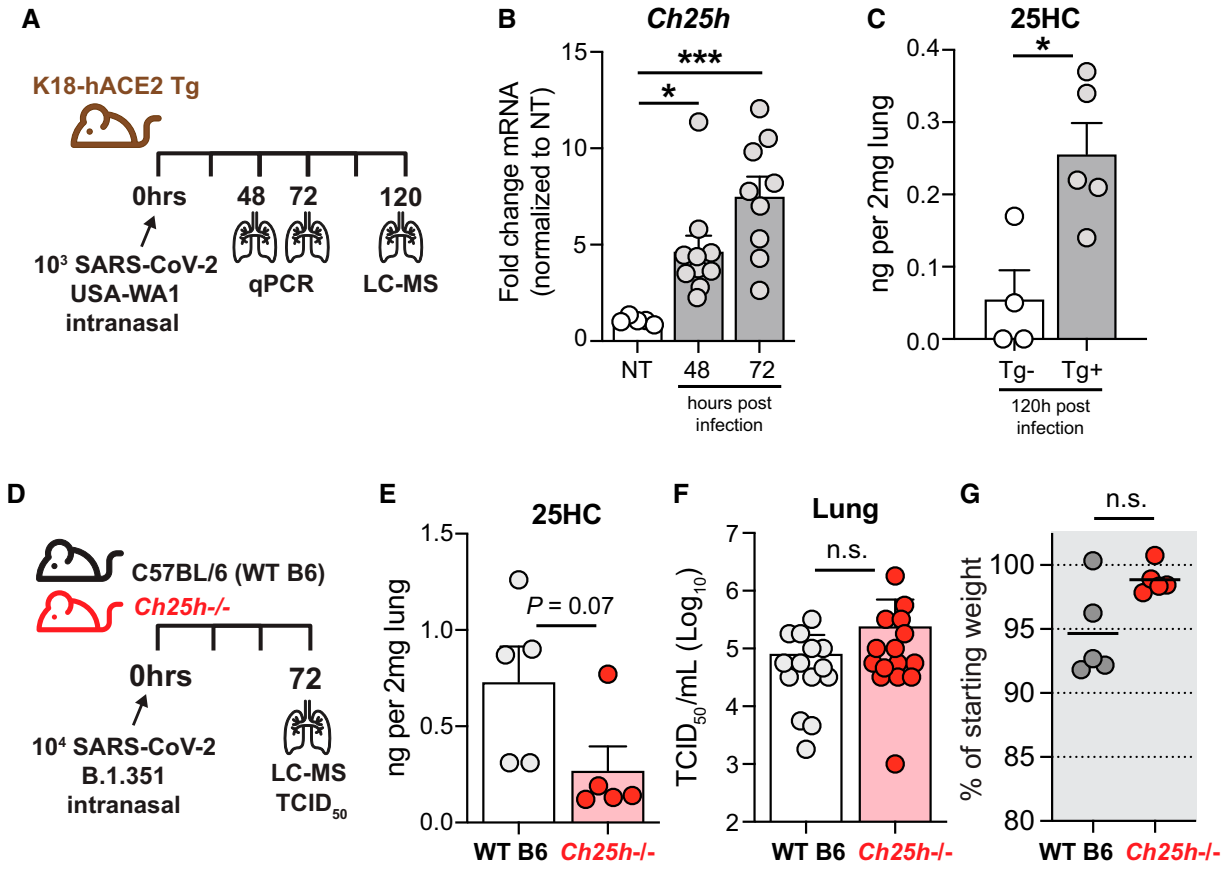

Figure 2. Cholesterol-25-hydroxylase (*Ch25h*) is induced by SARS-CoV-2 in mouse lung but does not regulate viral clearance. (*A*) K18–hACE2 (human angiotensin-converting enzyme 2) mice were left uninfected or infected with SARS-CoV-2 USA-WA1/2020. As per the scheme, *Ch25h* expression was quantified using quantitative polymerase chain reaction (qPCR) and 25HC using liquid chromatography–mass spectrometry (LC-MS) in lung homogenates at the indicated time points p.i. ($n = 4$–10 per condition). (*B*) Lung *Ch25h* expression by qPCR in mice left NT or infected with SARS-CoV-2 USA-WA1/2020. (*C*) K18-hACE2 (transgenic [Tg+]) mice or B6 (Tg−) mice, a negative control for infection, were exposed to SARS-CoV-2 USA-WA1/2020, and lung 25HC was quantified at 120 hours p.i. (*D*) WT (B6) or *Ch25h*$^{-/-}$ mice were infected with SARS-CoV2 B.1.351. As per the scheme, lung viral load was quantified using $TCID_{50}$ assay and lung 25HC using LC-MS at 72 hours p.i. ($n = 5$–15 per genotype). (*E*) Lung 25HC at 72 hours p.i. (*F*) Lung viral load at 72 hours p.i. (*G*) Weight change at 72 hours p.i. indexed to baseline weight ($n = 5$ per genotype). Data are mean ± SEM and are representative of two or three independent experiments. $^{*}P < 0.05$ and $^{***}P < 0.001$. NT = nontreated; p.i. = postinfection; $TCID_{50}$ = median tissue culture infectious dose; WT = wild-type.

action (29), did not change viral titers 3 days p.i. and was associated with only a modest increase in lung viral loads on Day 5 p.i., but there were no accompanying changes in body weight (Figure 6B). Similar results were obtained using a fivefold higher dose of inhibitor (not depicted). Taken together, these findings suggest that 7α,25HC- or EBI2-mediated immune functions do not have a significant impact on host defense during SARS-CoV-2 pneumonia in mice.

Discussion

During the past several years, 25HC has been shown to inhibit infection by several viruses through multiple mechanisms and thus has been proposed as a therapeutic candidate (3, 8, 30, 31). Reportedly, 25HC blocks viral fusion by reducing free cholesterol in host cell membranes (15, 17), a mechanism that may either involve direct membrane intercalation of 25HC or activation by 25HC of the cholesterol-esterifying enzyme acyl-coenzyme A:cholesterol acyltransferase (17). Additional antiviral mechanisms that have been proposed include inhibition of postentry gene expression (1, 14), activation of the nuclear receptor LXR (32), inhibition of the replication organelle through interactions with OSBP1 (oxysterol binding protein 1) (33), and activation of the integrated stress response (34). Although some of these mechanisms are proposed to involve direct binding interactions of 25HC with proteins (acyl-coenzyme A:cholesterol acyltransferase, OSBP1, LXR), other antiviral effects have been proposed to arise independently of 25HC–protein interactions (3). Our finding that 25HC had for more potent activity than ent-25HC against hCoV-229E suggests, consistent with a prior report (1), that 25HC is enantioselective, likely triggering protein-dependent effects at low concentrations that may be complemented by additional protein-independent mechanisms at higher concentrations.

Contrary to recent reports (14–17), we found no antiviral efficacy for 25HC against SARS-CoV-2 *in vitro*. This is despite our inclusion of 25HC concentrations higher than the half maximal effective concentration for SARS-CoV-2 reported in these other

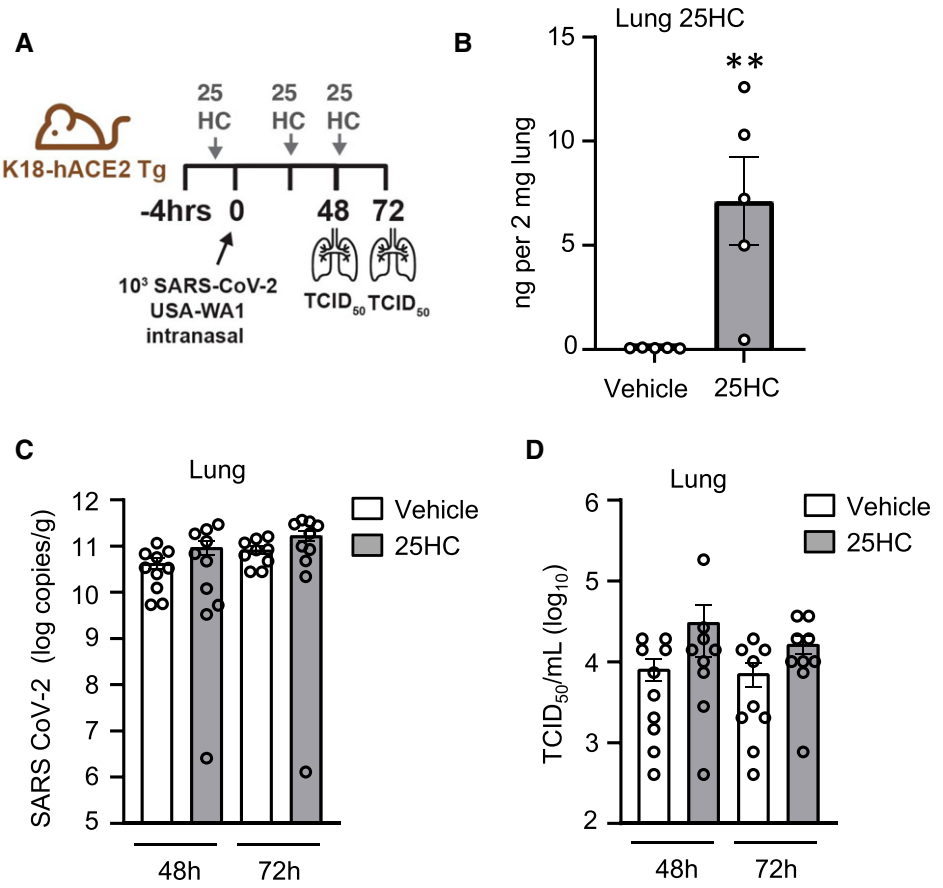

Figure 3. 25HC treatment does not modify viral clearance during SARS-CoV-2 pneumonia. (*A*) As shown in the schematic, K18-hACE2 mice were injected i.p. with 50 mg/kg/d 25HC (or vehicle) starting at −4 hours preceding i.n. inoculation with SARS-CoV-2, after which lungs were harvested at the indicated times p.i. (*B*) B6 mice received i.p. injections of 25HC or vehicle per *A*, and 25HC concentrations were measured using LC-MS in lung homogenates. (*C* and *D*) Lungs harvested at the indicated time points were evaluated for viral load using qPCR (*C*) or plaque assay (*D*). $n = 9$ or 10 per condition. Data are mean ± SEM. $^{**}P < 0.01$.

publications (3.675 μM [16], 4.2 μM [14]), concentrations that are unlikely to be easily achievable *in vivo*. Although we can only speculate on the reason for our different result, we presume that it reflects methodological differences, among them the choice of cell line (Calu-3, Caco-2 [17]; HEK293-hACE2 [15]) and virus strain (14, 15) and the timing of 25HC treatment (14). Although not all reports have specified the vehicle used, we found no antiviral effect of 25HC for SARS-CoV-2 in either DMSO or ethanol (not depicted). Although our data do not permit confident conclusions to be drawn about the relative susceptibility of SARS-CoV-2 and hCoV-229E to 25HC, there are several possibilities, both technical and biological. The antiviral effect of 25HC has recently been shown to be affected by plasma membrane cholesterol content (35). Our optimized *in vitro* assays for the two viruses used different FBS concentrations (2% for SARS-CoV-2, 10% for hCoV-229E), and it is possible that this could have caused different membrane cholesterol content. Alternatively, 25HC has been shown to inhibit some viruses by affecting expression and post-translational modification of viral proteins (3), and it is possible that hCoV-229E and SARS-CoV-2 may have differential susceptibility to these mechanisms.

In vivo, we also did not detect any effect of supplemental 25HC or CH25H deletion on multiple disease measures during SARS-CoV-2 pneumonia. Recently, it was reported that 25HC, delivered intragastrically at 100 mg/kg/d starting 1 day before infection, reduced lung viral load of the mouse-adapted SARS-CoV-2 strain MASCp6 in Balb/C mice (16). Technical differences, including 25HC dose, 25HC route, virus strain, and mouse strain, may possibly account for the divergence in our findings. Our dosing regimen (50 mg/kg/d i.p. in β-cyclodextrin vehicle) was previously reported to reduce HIV viral load in humanized mice (2) and to reduce Zika virus load and mortality in Balb/C mice (7). We have also previously shown that this 25HC regimen is therapeutic against lung inflammation by enhancing the efferocytic function of alveolar macrophages (5). This latter finding, taken together with the lung homogenate 25HC measurements in the present study (Figure 3B), suggests that systemically dosed 25HC penetrates the airspace in biologically active form. Further supporting this, it was recently reported that systemic treatment with 25HC improved survival and reduced viral load, inflammation, and injury in the lungs of pigs during pneumonia with the coronavirus porcine reproductive and respiratory syndrome virus (8). Our finding that lung 25HC concentrations were not abolished in *Ch25h*$^{-/-}$ mice (Figure 2) is consistent with reports that additional enzymes contribute to

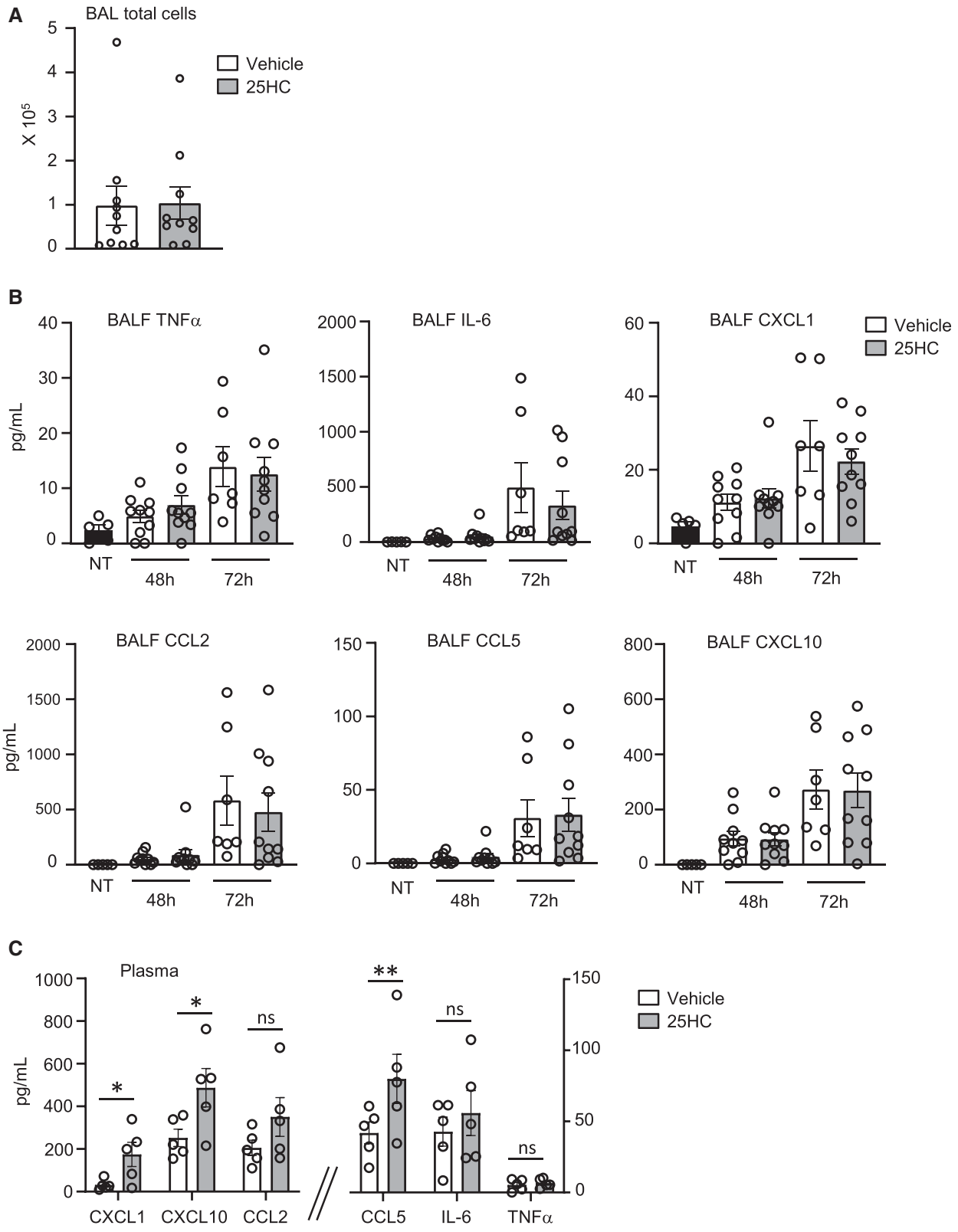

Figure 4. 25HC treatment does not modify the inflammatory response during SARS-CoV-2 pneumonia. K18-hACE2 mice were either left NT or injected i.p. with 50 mg/kg/d 25HC (or vehicle) starting at −4 hours preceding i.n. inoculation with SARS-CoV-2. (*A*) BAL cells were quantified 48 hours postinfection ($n = 10$ per treatment). (*B*) Cytokines and chemokines were quantified in BALF at 48 and 72 hours postinfection ($n = 5$–10 per condition). (*C*) Plasma cytokines and chemokines were quantified at 120 hours postinfection ($n = 5$ per treatment). Data are mean ± SEM. *$P < 0.05$; **$P = 0.08$. BALF = BAL fluid.

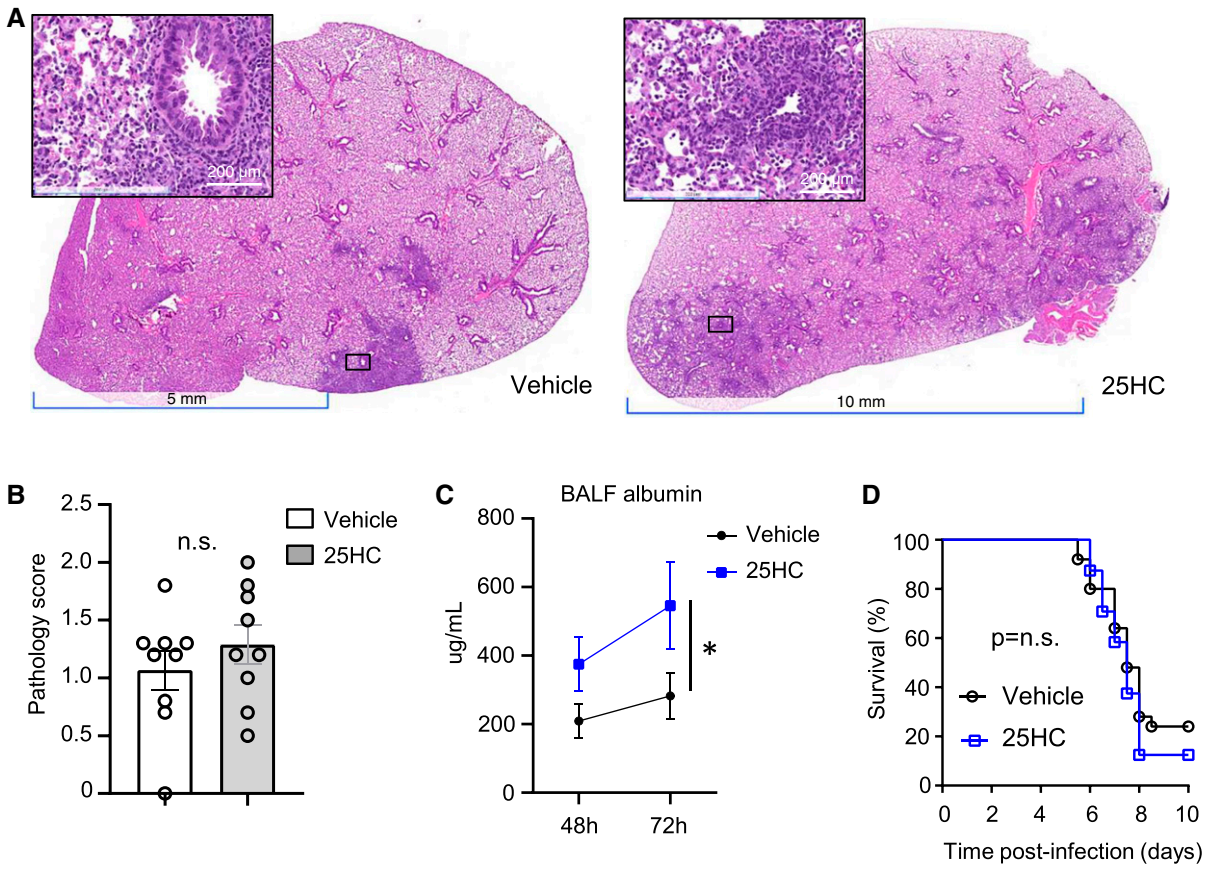

Figure 5. 25HC treatment does not modify lung histopathology or mortality during SARS-CoV-2 pneumonia. K18-hACE2 mice were injected i.p. with 50 mg/kg/d 25HC (or vehicle) starting at −4 hours preceding i.n. inoculation with SARS-CoV-2. Lungs were harvested on Day 5 p.i., fixed, stained with hematoxylin and eosin, and scored for histopathology. (*A* and *B*) Representative images (*A*) and composite pathology scores (*B*) are shown ($n = 9$ per condition). (*C*) BALF albumin, an indicator of microvascular injury, was measured at the indicated times p.i. ($n = 5$–10 per condition). Scale bars: *A* (left panel) 5 mm, (inset) 200 μm; *A* (right panel) 10 mm, (inset) 200 μm. (*D*) Survival was monitored ($n = 25$ per treatment). Data are mean ± SEM and are representative of two or three independent experiments.*$P < 0.05$.

25HC biosynthesis (26). It is possible that deletion or inhibition of these additional enzymes may be required to reduce endogenous 25HC to low enough concentrations to affect viral clearance. Future studies are also warranted to test whether Ch25h/25HC impacts late-phase resolution of virus-induced inflammation in the lung.

25HC is further oxidized by CYP7B1 on carbon-7, yielding the bioactive oxysterol 7α,25HC. Reportedly, 7α,25HC is depleted in *Ch25h*-null mice (27) and is generated in response to exogenous 25HC substrate (2), and it may regulate trafficking of immune cells to the lung in some settings (4, 6, 11, 12, 36). It is a limitation of the present study that we did not measure 7α,25HC concentrations in the SARS-CoV-2–infected lung. Nonetheless, we tested mice null for the 7α,25HC receptor EBI2 (encoded by *Gpr183*) in the SARS-CoV-2 pneumonia model to exclude possible confounding effects by this downstream lipid in our studies. We did not find any change in lung viral load in *Gpr183*$^{-/-}$ mice on Day 3 p.i. or alterations in body weight loss in EBI2 inhibitor–treated mice out to Day 5 p.i., suggesting that, at least at these early time points, 7α,25HC does not play a major role in anti–SARS-CoV-2 host defense. Although we have previously reported that eosinophil expression of GPR183 is dispensable for pulmonary migration after SARS-CoV2 infection (6), our studies here do not exclude the possibility that 7α,25HC and EBI2 may regulate infiltration of other immune cells into the infected lung parenchyma. Importantly, mice deficient in EBI2 mount defective T cell–dependent plasma cell and germinal center responses (27, 37), and thus the small increase in viral titers at Day 5, a time point when SARS-CoV-2–specific T-cell responses can be detected in the lungs of mice, may be related to possible defects in antiviral T- and B-cell responses during EBI2 inhibition. In contrast to our findings, a recent study using a 150-fold higher dose (7.6 mg/kg twice daily) of the EBI2 inhibitor NIBR189 reported a decrease in mouse-adapted SARS-CoV-2 viral titers at both Day 2 and Day 5 (38). Of note, although administration of the EBI2 inhibitor decreased viral loads in WT mice, mice deficient in GPR183 did not show changes in viral burden compared with WT mice, arguing that the mode of action of the EBI2 inhibitor NIBR189in this study does not recapitulate genetic absence of GPR183 (38).

The increase in 25HC-treated animals of BALF albumin, an established metric of pulmonary microvascular lung injury (18), suggests 25HC effect on the pulmonary

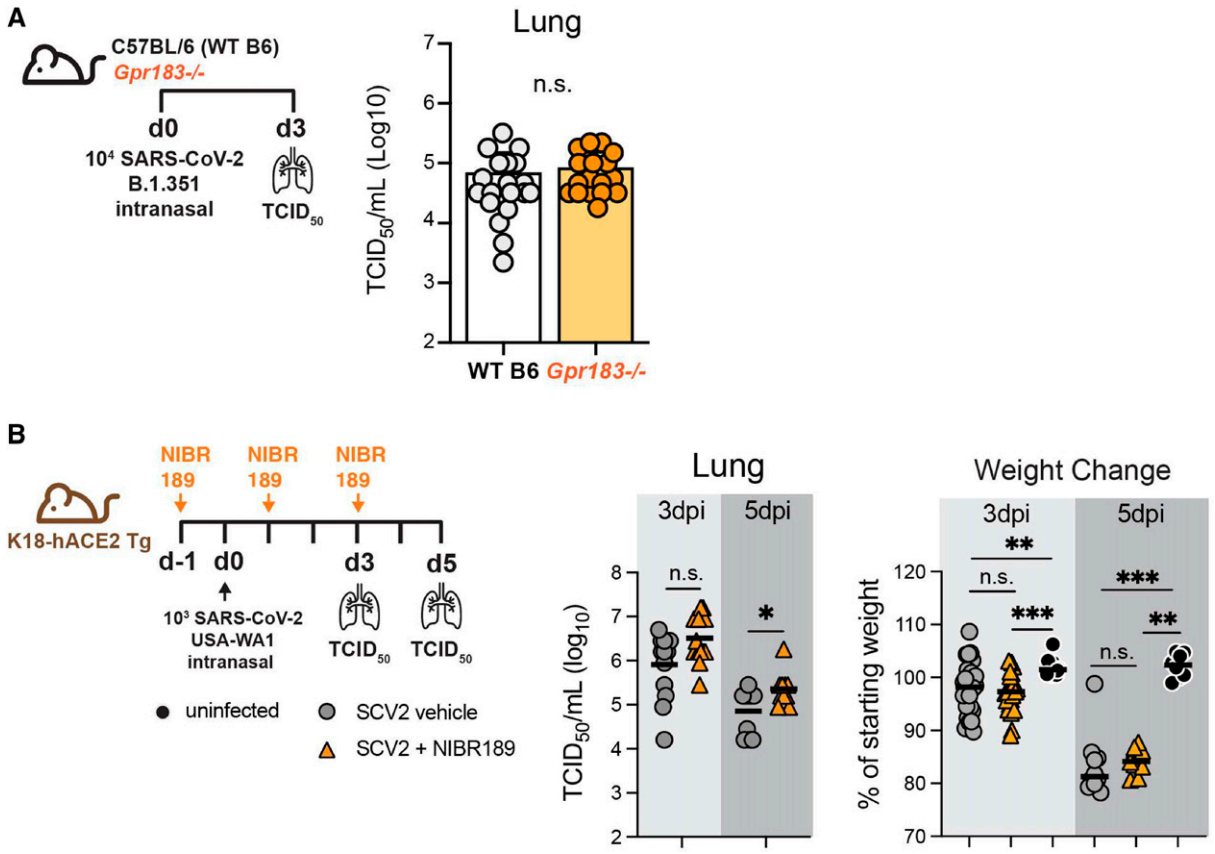

Figure 6. No effect of *Gpr183* (G protein–coupled receptor 183) deletion or EBI2 (Epstein-Barr virus–induced gene 2) inhibition on SARS-CoV-2 clearance or morbidity. (*A*) As per scheme at left, *Gpr183*$^{-/-}$ and WT (B6) mice were infected i.n. with a target dose of 3.5×10^4 SARS-CoV-2 B.1.351. Viral load in lung was quantified on Day 3 p.i. ($n = 18$ per genotype, three independent experiments) (right). (*B*) As per scheme at left, K18-hACE2 transgenic mice were either left uninfected or treated i.p. with 0.1 mg/kg EBI2 (encoded by *Gpr183*) inhibitor NIBR189 (or vehicle control) and infected i.n. with a target dose of 1×10^3 SARS-CoV2 USA-WA1/2020. Lung viral load (middle) and weight change (right) were quantified ($n = 7$–20/condition, two independent experiments per time point). Data are mean ± SEM. *$P < 0.05$, **$P < 0.01$, and ***$P < 0.001$. d = day; SCV2 = severe acute respiratory syndrome coronavirus 2.

endothelial barrier, a putative cellular target of SARS-CoV-2 (25). Reportedly, 25HC is cytotoxic to endothelial cells (39–41), and we recently reported that it exacerbates vascular leak in the lung after high-dose LPS inhalation (42). The elevated plasma cytokines we observed in 25HC-treated mice may also derive from endothelial cells, given prior reports that 25HC augments cytokine expression by endothelial cells (43). Future studies will be necessary to examine the effect of 25HC on pulmonary vascular biology in greater detail. One group recently reported that direct intratracheal instillation of 25HC reduces LPS-induced lung inflammation (44). Although this route might be expected to improve delivery to the alveolar epithelium and to reduce exposure of the endothelium compared with intraperitoneal injection, intratracheal aspiration is well known to yield highly patchy, heterogeneous deposition in the lung (45). Aerosol delivery reportedly provides superior alveolar delivery (45), but methods for aerosolization of 25HC have not been reported to our knowledge.

Conclusions

Although our findings suggest that caution is warranted in extrapolating from studies of 25HC in other viruses to SARS-CoV-2, we propose that further exploration is still warranted of strategies that deliver 25HC more selectively to the primary cellular target of infection, respiratory epithelial cells. Along these lines, formulation of 25HC with cationic lipid as nanovesicles was recently reported to significantly improve lung-selective targeting of systemically dosed 25HC (46). Additional emerging strategies, such as conjugation of 25HC to viral fusion inhibitory peptides (13), also warrant future investigation in SARS-CoV-2 pneumonia. Given that CH25H and 25HC are reportedly increased in patients with chronic obstructive pulmonary disease (4, 47) and in obese subjects (48), future studies to define the impact of native oxysterols on coronavirus disease (COVID-19) risk in lung disease (49) and in obesity (50) will also be of interest. ■

Author disclosures are available with the text of this article at www.atsjournals.org.

Acknowledgment: The authors are grateful to the staff of the NIAID Animal Biosafety Level 2 and 3 facilities and the NIAID SARS-CoV-2 Virology Core.

References

1. Blanc M, Hsieh WY, Robertson KA, Kropp KA, Forster T, Shui G, *et al.* The transcription factor STAT-1 couples macrophage synthesis of 25-hydroxycholesterol to the interferon antiviral response. *Immunity* 2013;38:106–118.
2. Liu SY, Aliyari R, Chikere K, Li G, Marsden MD, Smith JK, *et al.* Interferon-inducible cholesterol-25-hydroxylase broadly inhibits viral entry by production of 25-hydroxycholesterol. *Immunity* 2013;38:92–105.
3. Lembo D, Cagno V, Civra A, Poli G. Oxysterols: an emerging class of broad spectrum antiviral effectors. *Mol Aspects Med* 2016;49:23–30.
4. Jia J, Conlon TM, Sarker RS, Taşdemir D, Smirnova NF, Srivastava B, *et al.* Cholesterol metabolism promotes B-cell positioning during immune pathogenesis of chronic obstructive pulmonary disease. *EMBO Mol Med* 2018;10:e8349.
5. Madenspacher JH, Morrell ED, Gowdy KM, McDonald JG, Thompson BM, Muse G, *et al.* Cholesterol 25-hydroxylase promotes efferocytosis and resolution of lung inflammation. *JCI Insight* 2020;5:e137189.
6. Bohrer AC, Castro E, Tocheny CE, Assmann M, Schwarz B, Bohrnsen E, *et al.*; Tuberculosis Imaging Program. Rapid GPR183-mediated recruitment of eosinophils to the lung after *Mycobacterium tuberculosis* infection. *Cell Rep* 2022;40:111144.
7. Li C, Deng YQ, Wang S, Ma F, Aliyari R, Huang XY, *et al.* 25-Hydroxycholesterol protects host against Zika virus infection and its associated microcephaly in a mouse model. *Immunity* 2017;46:446–456.
8. Song Z, Bai J, Nauwynck H, Lin L, Liu X, Yu J, *et al.* 25-Hydroxycholesterol provides antiviral protection against highly pathogenic porcine reproductive and respiratory syndrome virus in swine. *Vet Microbiol* 2019;231:63–70.
9. Dang EV, McDonald JG, Russell DW, Cyster JG. Oxysterol restraint of cholesterol synthesis prevents AIM2 inflammasome activation. *Cell* 2017; 171:1057–1071.e11.
10. Gold ES, Diercks AH, Podolsky I, Podyminogin RL, Askovich PS, Treuting PM, *et al.* 25-Hydroxycholesterol acts as an amplifier of inflammatory signaling. *Proc Natl Acad Sci U S A* 2014;111: 10666–10671.
11. Ngo MD, Bartlett S, Bielefeldt-Ohmann H, Foo CX, Sinha R, Arachchige BJ, *et al.* A blunted GPR183/oxysterol axis during dysglycemia results in delayed recruitment of macrophages to the lung during *Mycobacterium tuberculosis* infection. *J Infect Dis* 2022;225: 2219–2228.
12. Shen ZJ, Hu J, Kashi VP, Kelly EA, Denlinger LC, Lutchman K, *et al.* Epstein-Barr virus-induced gene 2 mediates allergen-induced leukocyte migration into airways. *Am J Respir Crit Care Med* 2017;195: 1576–1585.
13. Lan Q, Wang C, Zhou J, Wang L, Jiao F, Zhang Y, *et al.* 25-Hydroxycholesterol-conjugated EK1 peptide with potent and broad-spectrum inhibitory activity against SARS-CoV-2, its variants of concern, and other human coronaviruses. *Int J Mol Sci* 2021;22:11869.
14. Yuan S, Chan CC, Chik KK, Tsang JO, Liang R, Cao J, *et al.* Broad-spectrum host-based antivirals targeting the interferon and lipogenesis pathways as potential treatment options for the pandemic coronavirus disease 2019 (COVID-19). *Viruses* 2020;12:628.
15. Zang R, Case JB, Yutuc E, Ma X, Shen S, Gomez Castro MF, *et al.* Cholesterol 25-hydroxylase suppresses SARS-CoV-2 replication by blocking membrane fusion. *Proc Natl Acad Sci U S A* 2020;117: 32105–32113.
16. Zu S, Deng YQ, Zhou C, Li J, Li L, Chen Q, *et al.* 25-Hydroxycholesterol is a potent SARS-CoV-2 inhibitor. *Cell Res* 2020;30:1043–1045.
17. Wang S, Li W, Hui H, Tiwari SK, Zhang Q, Croker BA, *et al.* Cholesterol 25-Hydroxylase inhibits SARS-CoV-2 and other coronaviruses by depleting membrane cholesterol. *EMBO J* 2020;39:e106057.
18. Kulkarni HS, Lee JS, Bastarache JA, Kuebler WM, Downey GP, Albaiceta GM, *et al.* Update on the features and measurements of experimental acute lung injury in animals: an official American Thoracic Society workshop report. *Am J Respir Cell Mol Biol* 2022;66:e1–e14.
19. Baptista AP, Gola A, Huang Y, Milanez-Almeida P, Torabi-Parizi P, Urban JF Jr, *et al.* The chemoattractant receptor Ebi2 drives intranodal naive $CD4^+$ T cell peripheralization to promote effective adaptive immunity. *Immunity* 2019;50:1188–1201.e6.
20. Liu X, Luongo C, Matsuoka Y, Park HS, Santos C, Yang L, *et al.* A single intranasal dose of a live-attenuated parainfluenza virus-vectored SARS-CoV-2 vaccine is protective in hamsters. *Proc Natl Acad Sci U S A* 2021;118:e2109744118.
21. Bauman DR, Bitmansour AD, McDonald JG, Thompson BM, Liang G, Russell DW. 25-Hydroxycholesterol secreted by macrophages in response to Toll-like receptor activation suppresses immunoglobulin A production. *Proc Natl Acad Sci U S A* 2009;106:16764–16769.
22. McDonald JG, Thompson BM, McCrum EC, Russell DW. Extraction and analysis of sterols in biological matrices by high performance liquid chromatography electrospray ionization mass spectrometry. *Methods Enzymol* 2007;432:145–170.
23. Weil T, Lawrenz J, Seidel A, Münch J, Müller JA. Immunodetection assays for the quantification of seasonal common cold coronaviruses OC43, NL63, or 229E infection confirm nirmatrelvir as broad coronavirus inhibitor. *Antiviral Res* 2022;203:105343.
24. Winkler ES, Bailey AL, Kafai NM, Nair S, McCune BT, Yu J, *et al.* SARS-CoV-2 infection of human ACE2-transgenic mice causes severe lung inflammation and impaired function. *Nat Immunol* 2020;21:1327–1335.
25. Lei Y, Zhang J, Schiavon CR, He M, Chen L, Shen H, *et al.* SARS-CoV-2 spike protein impairs endothelial function via downregulation of ACE 2. *Circ Res* 2021;128:1323–1326.
26. Cyster JG, Dang EV, Reboldi A, Yi T. 25-Hydroxycholesterols in innate and adaptive immunity. *Nat Rev Immunol* 2014;14:731–743.
27. Hannedouche S, Zhang J, Yi T, Shen W, Nguyen D, Pereira JP, *et al.* Oxysterols direct immune cell migration via EBI2. *Nature* 2011;475: 524–527.
28. Chalmin F, Rochemont V, Lippens C, Clottu A, Sailer AW, Merkler D, *et al.* Oxysterols regulate encephalitogenic $CD4^+$ T cell trafficking during central nervous system autoimmunity. *J Autoimmun* 2015;56: 45–55.
29. Smirnova NF, Conlon TM, Morrone C, Dorfmuller P, Humbert M, Stathopoulos GT, *et al.* Inhibition of B cell-dependent lymphoid follicle formation prevents lymphocytic bronchiolitis after lung transplantation. *JCI Insight* 2019;4:e123971.
30. Zhang Y, Song Z, Wang M, Lan M, Zhang K, Jiang P, *et al.* Cholesterol 25-hydroxylase negatively regulates porcine intestinal coronavirus replication by the production of 25-hydroxycholesterol. *Vet Microbiol* 2019;231:129–138.
31. Fessler MB. The intracellular cholesterol landscape: dynamic integrator of the immune response. *Trends Immunol* 2016;37:819–830.
32. Liu Y, Wei Z, Zhang Y, Ma X, Chen Y, Yu M, *et al.* Activation of liver X receptor plays a central role in antiviral actions of 25-hydroxycholesterol. *J Lipid Res* 2018;59:2287–2296.
33. Roulin PS, Lötzerich M, Torta F, Tanner LB, van Kuppeveld FJ, Wenk MR, *et al.* Rhinovirus uses a phosphatidylinositol 4-phosphate/cholesterol counter-current for the formation of replication compartments at the ER-Golgi interface. *Cell Host Microbe* 2014;16: 677–690.
34. Shibata N, Carlin AF, Spann NJ, Saijo K, Morello CS, McDonald JG, *et al.* 25-Hydroxycholesterol activates the integrated stress response to reprogram transcription and translation in macrophages. *J Biol Chem* 2013;288:35812–35823.
35. Heisler DB, Johnson KA, Ma DH, Ohlson MB, Zhang L, Tran M, *et al.* A concerted mechanism involving ACAT and SREBPs by which oxysterols deplete accessible cholesterol to restrict microbial infection. *eLife* 2023;12:e83534.
36. Fessler MB. Regulation of adaptive immunity in health and disease by cholesterol metabolism. *Curr Allergy Asthma Rep* 2015;15:48.
37. Liu C, Yang XV, Wu J, Kuei C, Mani NS, Zhang L, *et al.* Oxysterols direct B-cell migration through EBI2. *Nature* 2011;475:519–523.
38. Foo CX, Bartlett S, Chew KY, Ngo MD, Bielefeldt-Ohmann H, Arachchige BJ, *et al.* GPR183 antagonism reduces macrophage infiltration in influenza and SARS-CoV-2 infection. *Eur Respir J* 2023;61:2201306.
39. Chalubinski M, Zemanek K, Skowron W, Wojdan K, Gorzelak P, Broncel M. The effect of 7-ketocholesterol and 25-hydroxycholesterol on the integrity of the human aortic endothelial and intestinal epithelial barriers. *Inflamm Res* 2013;62:1015–1023.
40. Lizard G, Deckert V, Dubrez L, Moisant M, Gambert P, Lagrost L. Induction of apoptosis in endothelial cells treated with cholesterol oxides. *Am J Pathol* 1996;148:1625–1638.

41. Ou ZJ, Chen J, Dai WP, Liu X, Yang YK, Li Y, *et al.* 25-Hydroxycholesterol impairs endothelial function and vasodilation by uncoupling and inhibiting endothelial nitric oxide synthase. *Am J Physiol Endocrinol Metab* 2016;311:E781–E790.
42. Madenspacher JH, Morrell ED, McDonald JG, Thompson BM, Li Y, Birukov KG, *et al.* 25-Hydroxycholesterol exacerbates vascular leak during acute lung injury. *JCI Insight* 2023;8:e155448.
43. Morello F, Saglio E, Noghero A, Schiavone D, Williams TA, Verhovez A, *et al.* LXR-activating oxysterols induce the expression of inflammatory markers in endothelial cells through LXR-independent mechanisms. *Atherosclerosis* 2009;207:38–44.
44. Bottemanne P, Paquot A, Ameraoui H, Guillemot-Legris O, Alhouayek M, Muccioli GG. 25-Hydroxycholesterol metabolism is altered by lung inflammation, and its local administration modulates lung inflammation in mice. *FASEB J* 2021;35:e21514.
45. Brain JD, Knudson DE, Sorokin SP, Davis MA. Pulmonary distribution of particles given by intratracheal instillation or by aerosol inhalation. *Environ Res* 1976;11:13–33.
46. Kim H, Lee HS, Ahn JH, Hong KS, Jang JG, An J, *et al.* Lung-selective 25-hydroxycholesterol nanotherapeutics as a suppressor of COVID-19-associated cytokine storm. *Nano Today* 2021;38:101149.
47. Sugiura H, Koarai A, Ichikawa T, Minakata Y, Matsunaga K, Hirano T, *et al.* Increased 25-hydroxycholesterol concentrations in the lungs of patients with chronic obstructive pulmonary disease. *Respirology* 2012; 17:533–540.
48. Russo L, Muir L, Geletka L, Delproposto J, Baker N, Flesher C, *et al.* Cholesterol 25-hydroxylase (CH25H) as a promoter of adipose tissue inflammation in obesity and diabetes. *Mol Metab* 2020;39: 100983.
49. Fessler MB. A new frontier in immunometabolism: cholesterol in lung health and disease. *Ann Am Thorac Soc* 2017;14:S399–S405.
50. Suratt BT, Ubags NDJ, Rastogi D, Tantisira KG, Marsland BJ, Petrache I, *et al.*; Allergy, Immunology, and Inflammation Assembly. An official American Thoracic Society workshop report: obesity and metabolism. An emerging frontier in lung health and disease. *Ann Am Thorac Soc* 2017;14:1050–1059.